Numerical investigation of direct absorption solar collectors based on carbon black nanofluids

Shihao Wei[1, b)], Boris V. Balakin[2, c)], Pawel Kosinski[1, a)]

[1]University of Bergen, Department of Physics and Technology, Bergen, Norway
[2]Western Norway University of Applied Sciences, Department of Mechanical and Marine Engineering, Bergen, Norway

[a)] Corresponding author: pawel.kosinski@uib.no
[b)] shihao.wei@uib.no
[c)] boris.balakin@hvl.no

Abstract. A novel model of a rectangular direct absorption solar collector (DASC) based on carbon black (CB) nanofluids for concentrated solar power is presented herein. Distributions of temperature, velocity, volume fraction of nanofluid were analyzed as well as the effect of CB concentration. A mesh independence study was also conducted. The results show that the optimal temperature and efficiency were, respectively, 331.669 K and 0.7234, for the concentration of 0.05 wt. %. The main reason was that higher concentration of CB formed a "shield" that blocked the light. The distribution of temperature and velocity of the nanofluid, and the volume fraction of carbon black during the flow process were highlighted. The study reveals that the nanoparticle has huge potential to improve the efficiency of DASC.

INTRODUCTION

Nanofluids are colloidal suspensions of nanometer-sized particles [1]. Owing to their improved thermal proportions to the base fluid, nanofluids are considered to be excellent absorption fluids for solar collectors [2]. Many researchers investigated the performance of nanofluids in different solar collectors. Saidur [3] conducted a numerical study on the thermal performance in a flat plate solar collector (FPSC). The results show that the exergy efficiency increased with an increasing of the volume fraction of nanoparticles in fluid. Mwesigye et al. [4] numerically investigated the performance of a parabolic trough solar collector (PTSC) exploiting carbon nanotubes - Therminol VP-1 based nanofluid. The heat transfer performance increased about 234% when using the nanofluid and the thermal efficiency enhanced about 4.4% as the volume fraction of the nanoparticle increased from 0 to 2.5%. Gorji and Ranjbar [5] conducted a numerical and experimental study on a direct absorption solar collector (DASC) using graphite, magnetite and silver nanofluids as base fluid. The result revealed that the maximum enhancement of exergy efficiency was 20.3% with magnetite nanofluid compared to other base fluids. Their numerical study showed that the outlet temperature of DASC increases with increase in the nanofluid concentration at a constant flow rate and solar flux.

Comparing to other types of solar collector, DASC utilizes fluid as the absorbing medium for incident sunlight as compared to a solid absorber, and it can provide an increase of efficiency compared to the indirect collector [6]. Various parameters can affect the efficiency of DASC. Tyagi et al. [7] evaluated the effect of geometrical parameters on the performance of DASC using an aluminum nanofluid. The results showed that the efficiency increased with the collector length first and then decreased. Sharaf et al. [8] investigated the collector optical behavior using a suspension of graphite nanoparticles in two different base fluids including water and Therminol VP-1. It was found that the extinction coefficient of the nanofluid using the base fluid of water was higher than that of Therminol VP-1 at high nanofluid concentrations. According to the experimental and numerical study conducted by Delfani et al. [9], the fluid absorption coefficient and the outlet temperature increased by increasing MWCNT (multi-walled carbon nanotubes) nanofluid volume fraction at constant flow rate. Furthermore, the efficiency enhancement of 9%, 13.1%, 21.6% and 27.4% was obtained for the volume fractions of 25 ppm, 50 ppm and 100 ppm compared with that of using the base fluid as a working fluid.

In this research, we used CB based nanofluid as base fluid to investigate a rectangle collector with three baffles for the direct sunlight absorption, showing the fluid behaviour and deposition of nanoparticles. As a key factor of a DASC, the efficiency of the system was compared with the experimental results and some typical commercial model. To the authors' knowledge, this study is the first that investigates a multiphase computational fluid dynamics (CFD) model in in DASCs.

METHODOLOGY

Geometry and boundary conditions

The computational domain had a rectangular shape with three baffles, as shown in Figs. 1-2. The length of the domain was 0.39 m, the width was 0.23 m, and the depth was 0.02 m. The length of the baffles was 0.1475 m, and their width was 0.02 m. The flowrate was 2.0 litre/min, and the initial temperature was 40°C. The fluid entered the domain via a small pipe located in the lower left corner in Fig. 1. The inlet boundary condition was set there. The pressure outlet boundary was located symmetrically in the right side. The system was subjected to irradiation (from the bottom) by the intensity of 2000 W/m^2 with distance of 21 cm. We analyzed the intensity distribution and deduced the average intensity as 1103 W/m^2 All the surfaces were set as adiabatic apart from the inlet, outlet and the bottom surface. The geometry corresponded to the DASC researched by Espedal [10].

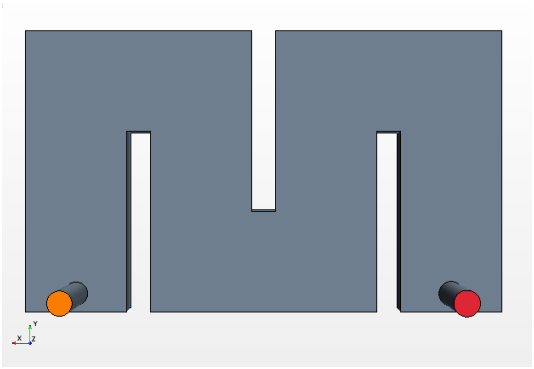

Fig. 1 Geometry

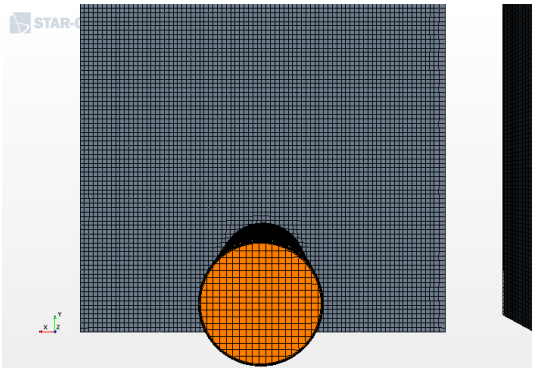

Fig. 2 Mesh

Governing equations

We consider an unsteady incompressible flow, described by the Navier-Stokes equations. The continuity equation reads [11]:

$$\frac{D(\alpha_i \rho_i)}{Dt} = 0, \tag{1}$$

where $\frac{D}{Dt}$ is the substantial derivative, α_i is the volume fraction, and ρ_i is the density. Subscript i denotes the difference phases where $i = p$ for the nanoparticle and $i = f$ for the base fluid.

The momentum equation is given by [12]:

$$\frac{D(\alpha_i \rho_i \boldsymbol{v}_i)}{Dt} = \alpha_i \nabla p + \nabla \cdot (\alpha_i \mu_i \nabla \boldsymbol{v}_i) + \alpha_i \rho_i \boldsymbol{g} + \boldsymbol{F}_{D,ij}, \tag{2}$$

where $\boldsymbol{v}_i$ is the velocity vector, p is the pressure, μ is the dynamic viscosity, $\boldsymbol{g}$ is the acceleration due to gravity and $\boldsymbol{F}_{D,ij}$ is the drag force.

The drag force was computed as follows [13]:

$$\boldsymbol{F}_{D,ij} = \frac{\pi d^2}{8} n_p \rho_l C_D |\boldsymbol{v}_i - \boldsymbol{v}_j| (\boldsymbol{v}_i - \boldsymbol{v}_j), \tag{3}$$

where n_p is the number density of the nanoparticles, d is the diameter of the carbon black, and C_D is the drag coefficient computed using the standard expression by Schiller- Naumann [14].

The energy equation is given by [15]:

$$\frac{D(\alpha_i \rho_i e_i)}{Dt} = \nabla(\alpha_i \rho_i \nabla T_i) - q_{ij} + \alpha_i q_v, \tag{4}$$

where $\boldsymbol{e}_i = C_{p,i}T_i$ is the phase-specific enthalpy, and q_{ij} is the inter-phase heat transfer term. With the assumption that the convective heat transfer is established between the phases, the inter-phase heat transfer term is computed according to Ranz-Marshall. Furthermore, q_v is the volumetric heat generation due to absorption. We also assume that the heat loss only occurred at the bottom surface by convection and radiation.

We simplified the thermal re-radiation behavior by assuming that it only occurred at the bottom surface of the DASC. Also, we neglected emission and scattering terms for the light in the fluid. Thus, the volumetric heat transfer can be deduced from the Beer-Lambert equation:

$$q_{v,\ i} = I_R k_i \exp\left(-k_{nf} l\right) \tag{5}$$

where l is the length of the light path, I_R is the heat flux of the incident light acting of the top surface, k_i is the extinction coefficient of carbon black or water, k_{nf} is the extinction coefficient of nanofluid according to our separate experimental tests. We measured the absorptance for different concentration of nanofluids with different depth, and fit the average extinction coefficient by Beer-Lambert law.

Efficiency

The efficiency of a solar thermal collector is the ratio of collected thermal energy to the total incident energy:

$$\eta = \frac{C\dot{m}(T_{out} - T_{in})}{qA} \tag{8}$$

where η is the efficiency, C is the specific heat of nanofluids, $\dot{m}$ is the mass flow rate of the fluid in the collector, T_{out} and T_{in} are the temperatures of the nanofluid at the outlet and inlet, respectively, q is the solar irradiance and A is the solar collector surface area.

We study the effects on the collector efficiency of the two parameters: the solar intensity and CB concentration.

Equations (1) – (5) were solved using the commercial CFD program STAR-CCM+ 15.02.007. The numerical solution was obtained using an implicit SIMPLE (Semi-Implicit Method for Pressure Linked Equations) method, and the following relaxation coefficients were applied: 0.3 for pressure, 0.7 for velocity, 0.5 for phase volume fraction, 0.9 for the enthalpy, and 0.8 for the turbulence model. The governing equations were discretized temporally with the second order Euler technique marching by 1.0 ms. The upwind scheme was applied for spatial discretization [11].

Model validation

Espedal [10] investigated experimentally the photothermal performance of a rectangle DASC that consisted of three main elements: a glass surface, an inner plate structure with baffles, and an external aluminum box with hose connectors. In the present research, simulations based on the proposed model with the base fluid and CB nanofluid were conducted. The results were compared with the experimental results. When the flow rate was 2.0 L/min, and CB concentration was 0.05 wt.%, the efficiency was 0.7356 according to our simulations. The error was 1.35 % if compared with the experimental result equal to 0.7455 [10]. This indicates that the proposed model can be used to analyze the photothermal performance of the DASC.

RESULTS AND DISCUSSION

Fluid temperature and velocity distribution

Figs. 3-4 show distributions of nanofluid temperature and velocity on the bottom surface, respectively. At the inlet, the temperature was low and different coherent structures in the flow occurred because of the sudden change of the cross-section radius and flow direction. When the fluid passed the first baffle, the temperature increased, and the velocity direction became clearly defined. The maximum temperature occurred near the second baffle, and the flow showed a clear path to the outlet. By comparing Fig. 3 and Fig. 4, we see that the area with the higher velocity tended to have a lower temperature. This can be explained by the heat transfer by convection in this area: the higher the flow velocity, the more the heat

was transferred. The presence of the baffles increased the residence time of the nanofluid inside the DASC and, thus, made it possible to extend the duration of absorption. As one can notice, because of the inertia force, the maximum velocity did not show in the center of pipeline instead of on the right side of the centre. Therefore, the areas on the opposite side of the baffles had higher temperature. It is worth to emphasize that there was a displacement in these high temperature areas of the fluid towards the top surface (perpendicular to the figures) [8]. This phenomenon can be confirmed by Fig. 5 and Fig. 6 that show the volume fraction distribution at the bottom and top surface. At the bottom surface, the volume fraction distribution resembles the velocity field. However, no deposit of particles occurred in the low velocity regions (compare Fig. 3 with Fig. 5). This is caused by the heat flow towards the interior of the fluid volume. The temperature of the bottom surface was namely higher than inside the system. Fig. 6 shows the particle distribution on the top surface. This surface was set as an adiabatic wall. Thus, a higher particle volume fraction was observed close to the baffles.

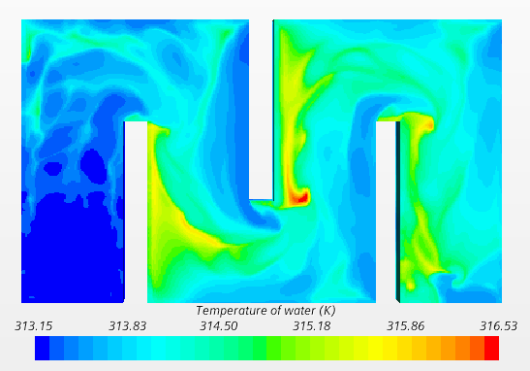

Fig. 3 Temperature distribution

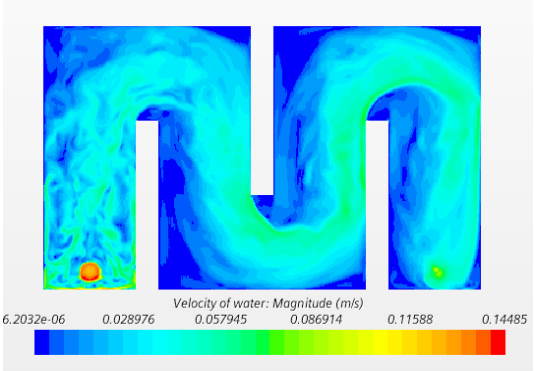

Fig. 4 Velocity distribution

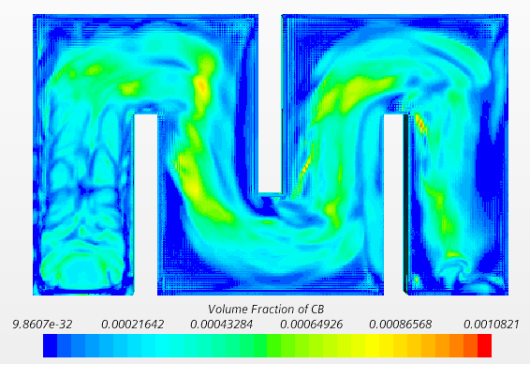

Fig. 5 CB volume fraction distribution (bottom)

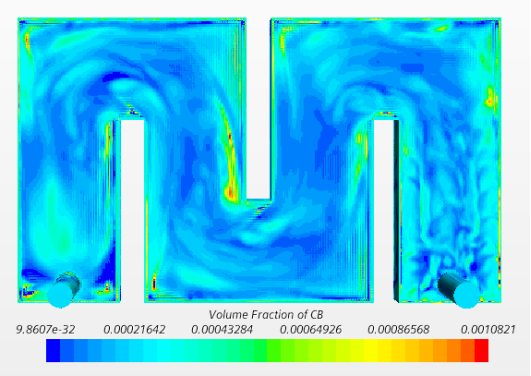

Fig. 6 CB volume fraction distribution (top)

These facts could potentially assist in increasing of the efficiency of the DASC for a commercial use. The higher temperature means the DASCs are more effective, but they are also accompanied by higher heat losses. Therefore, this should be considered when designing DASCs, by e.g., considering thermal insulation if possible.

Mesh independence study

Fig. 7 shows the thermal efficiencies of the system calculated for different cell mesh sizes. There is a slight decreasing tendency in the efficiency due to the increase of the cell mesh size. For larger computational cells, the results are less correct especially close to the system boundaries where steep temperature gradients occur. As a result, the temperature in the cells at the very boundary is too high. This results in a higher heat loss, i.e., a lower thermal efficiency.

Effect of CB concentration

Fig. 8 shows the thermal efficiency and outlet temperature for different CB concentrations for the cell mesh size of 1 mm. It can be seen from the figure that the efficiency and the outlet temperature increase with the CB concentration, and reach the maximum of 0.7656 and 313.669 K, respectively. This maximum occurs at CB concentration of 0.05 wt.%. The nanoparticles enhance the absorption of solar

radiation of the base flow. However, as the CB concentration increases further, the efficiency and the temperature decrease. When the number of nanoparticles in the base flow is low, the solar light can penetrate the nanofluid and reach the upper surface of the DASC easily. Hence, the fluid layer near the upper surface can also absorb the heat. This results in a more uniform temperature distribution and a low temperature gradient between the fluid layers. However, when the concentration is too high, there is a large number of nanoparticles that can form a "shield" at the bottom surface that block the solar light. As a result, only a thin layer of the nanoparticles can absorb the solar radiation directly, and the heat transfer is lower at these concentrations compared to low concentrations within the nanofluid. In this situation, there will also be a larger temperature gradient in these concentrations. Besides, as it can be anticipated, there will be higher temperature at the bottom surface and a lower temperature inside the system, compared to low concentrations, because the large number of nanoparticles can absorb more radiation. In our simulation model, all the surfaces were set as adiabatic except the bottom surface, so the heat loss only occurs at the outer layer of this surface. Therefore, the high temperature leads to more heat loss, and less heat transfer towards the fluid interior, so that there will be more heat loss to the surrounding. This results in a decrease of the outlet temperature and efficiency. It should be noted that the bottom surface was sealed by glass in the experiments [7]. There must have been an optical loss due to light reflection and absorption of glass. Therefore, the actual efficiency and temperature are lower than from the simulation results.

Similar results were obtained by some researchers. Otanicar et al. [17] studied the performance of a micro-DASC using an experimental setup and the aqueous suspensions containing silver and graphite nanoparticles and carbon nanotubes as the working fluids. The results show that the collector efficiency enhances by increase of nanofluid volume fraction, because the solar absorption of nanofluid increases. However, this increase continues to a certain amount of volume fraction, and then the reflection of solar radiation from the nanofluid increases, which results in the efficiency reduction.

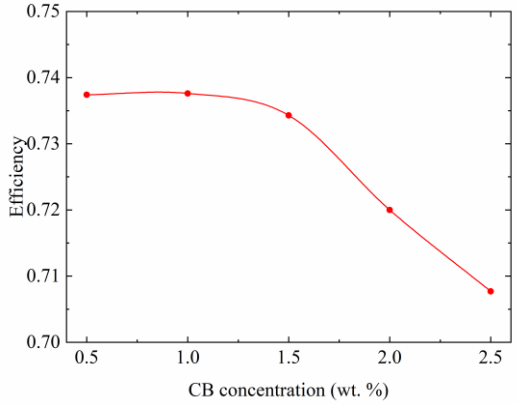

Fig. 7 Results of the mesh independence study

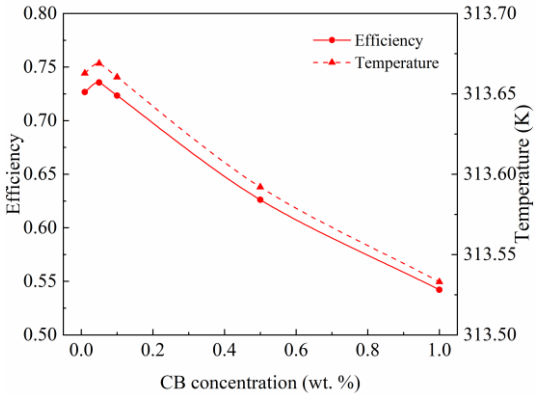

Fig.8 Efficiency for different CB concentrations

CONCLUSIONS AND FUTURE WORK

A CFD model of rectangular DASC was used to analyze the optical properties of CB nanoparticles and parameters of the DASC. According to the results, CB nanoparticles can increase the absorption of solar radiation of the base flow and the efficiency of the DASC. With the CB concentration increases, the outlet temperature and efficiency show the tendency of increasing first and then decreasing. Both the outlet temperature and the efficiency become optimal for the CB concentration of 0.05 wt. %. Moreover, the efficiency decreases with the mesh size because the lager mesh size induced the higher temperature difference between adjacent cells. According to the temperature and velocity distributions, there will be low flow velocity but high temperature zone in the rectangular DASC that can lead to a heat loss. Besides, CB nanoparticles will deposit at this zone. These reveal the potential improvement for the DASC to avoid the thermal loss.

Optimizing the numerical model is the first goal of the future work. As follows from our experience, the geometry and tile angle of DASC have significant effects on the performance of the DASC. Therefore, in the future, the efficiencies for different nanofluids and different geometries of DASCs should be considered.

ACKNOWLEDGMENTS

The computations were performed on resources provided by UNINETT Sigma2 - the National Infrastructure for High Performance Computing and Data Storage in Norway.

Boris Balakin thanks the Norwegian Research Council for funding (project 300286)

REFERENCES

1. Mahian, Omid, Kianifar, Ali, Kalogirou, Soteris A., Pop, Ioan, Wongwises, Somchai, 2013. *Int. J. Heat Mass Transf.* 57(2), 582–594.
2. Saidur, R., Leong, K.Y., Mohammad, H.A., 2011. Renew. Sustain. Energy Rev. 15 (3), 1646–1668.
3. Said, Z., Saidur, R., Rahim, N.A. and Alim, M.A., 2014.. *Energy and Buildings*, *78*, pp.1-9.
4. Mwesigye, A., Yılmaz, İ.H. and Meyer, J.P., 2018. *Renewable Energy*, *119*, pp.844-862.
5. Gorji, T.B. and Ranjbar, A.A., 2016*Solar Energy*, *135*, pp.493-505.
6. Li, Calvin H., Peterson, G.P., 2006. J. Appl. Phys. 99 (8), 084314.
7. Tyagi, H., Phelan, P. and Prasher, R., 2009. *Journal of solar energy engineering*, *131*(4).
8. Sharaf, O.Z., Kyritsis, D.C., Al-Khateeb, A.N. and Abu-Nada, E., 2018*Solar Energy*, *164*, pp.210-223.
9. Delfani, S., Karami, M. and Akhavan-Behabadi, M.A., 2016. *Renewable Energy*, *87*, pp.754-764.
10. Espedal, Lisbeth. Design and Experimental Studies of a Nanofluid Direct Absorption Solar Collector. MSc thesis. University of Bergen, 2020.
11. Bårdsgård, R., Kuzmenkov, D.M., Kosinski, P. and Balakin, B.V., 2020. *Journal of Renewable and Sustainable Energy*, *12*(3), p.033701.
12. Balakin, B.V., Zhdaneev, O.V., Kosinska, A. and Kutsenko, K.V., 2019. *Renewable Energy*, *136*, pp.23-32.
13. Struchalin, P.G., Yunin, V.S., Kutsenko, K.V., Nikolaev, O.V., Vologzhannikova, A.A., Shevelyova, M.P., Gorbacheva, O.S. and Balakin, B.V., 2021. *International Journal of Heat and Mass Transfer*, *179*, p.121717.
14. Fuchs, N.A., 1964. The Mechanics of Aerosols Pergamon Press. *New York*.
15. Kalteh, M., Abbassi, A., Saffar-Avval, M. and Harting, J., 2011. *International journal of heat and fluid flow*, *32*(1), pp.107-116.
16. Simonetti, M., Restagno, F., Sani, E., & Noussan, M. (2020). Solar Energy, 195, 166-175.
17. Otanicar, T.P., Phelan, P.E., Prasher, R.S., Rosengarten, G. and Taylor, R.A., 2010. *Journal of renewable and sustainable energy*, *2*(3), p.033102.